Reduction of [Re(X)(CO)$_3$(R′-DAB)] (X = Otf$^-$, Br$^-$; DAB = Diazabutadiene; R′ = iPr, pTol, pAn) and [Re(R)(CO)$_3$(iPr-DAB)] (R = Me, Et, Bz) Complexes: A Comparative (Spectro)electrochemical Study at Variable Temperatures

Brenda D. Rossenaar, František Hartl*, and Derk J. Stufkens

Anorganisch Chemisch Laboratorium, J. H. van't Hoff Research Institute, Universiteit van Amsterdam, Nieuwe Achtergracht 166, 1018 WV Amsterdam, The Netherlands

Received January 26, 1996[⊗]

This article describes the reduction routes of the complexes [Re(X)(CO)$_3$(R′-DAB)] (X = Br$^-$, Otf$^-$; R′ = pAn, pTol, iPr) and the metal−alkyl complexes [Re(R)(CO)$_3$(iPr-DAB)] (R = Me, Et, Bz), using data obtained from IR and UV−vis spectroelectrochemical measurements and cyclic voltammetry at variable temperatures. One-electron reduction of the complexes [Re(Br)(CO)$_3$(R′-DAB)] in nPrCN results in the establishment of an equilibrium between the radical anions [Re(Br)(CO)$_3$(R′-DAB)]$^{\bullet-}$ and the solvento radical [Re(nPrCN)(CO)$_3$(R′-DAB)]$^{\bullet}$. The ratio between these radical species could be tuned by changing the character of the R′ substituents on the R′-DAB ligand and by variation of the temperature. The radicals could be reduced in a subsequent one-electron step to give the five-coordinate anions [Re(CO)$_3$(R′-DAB)]$^-$ together with the six-coordinate anions [Re(nPrCN)-(CO)$_3$(R′-DAB)]$^-$ as the minor products. The bonding properties of the five-coordinate anions are discussed on the basis of a qualitative MO scheme and compared with those of the related complex [Mn(CO)$_3$(iPr-DAB)]$^-$. The main feature of the [Re(CO)$_3$(R′-DAB)]$^-$ complexes is a strong delocalization of their HOMOs, which rules out application of the localized-valence concept in this case. The complexes [Re(R)(CO)$_3$(iPr-DAB)] were found to be reduced in an electrochemically and chemically reversible one-electron step to give radical anionic products, tentatively formulated as {[Re(CO)$_3$(iPr-DAB)]$^-$···R$^{\bullet}$}. The radical nature of the products has been confirmed by ESR spectroscopy whereas the IR and UV−vis data correspond with the presence of the [Re(CO)$_3$(iPr-DAB)]$^-$ moiety.

Introduction

The complexes [Re(L′)(CO)$_3$(α-diimine)]$^{+/0}$ (L′ = halide, bridging ligand, organic donor, *etc.*) have received considerable attention[1−3] because of their ability to mediate energy and electron transfer reactions and to act as catalysts for CO_2 reduction.[4−17] Previous investigations revealed that organometallic electrocatalysts generally provide in their reduced state one vacant site for CO_2 coordination. The pentacoordinate radicals and anions, formed upon reduction of [Re(L′)(CO)$_3$-(α-diimine)]$^{+/0}$ complexes, have been recognized as suitable candidates for this purpose.[9,11,12] A systematic study of the electrochemistry of transition metal carbonyls with an α-diimine ligand, thereby varying the α-diimine ligands, coligands, and the metal center, can help with a formulation of criteria for the design of an active catalyst.[11,12] Spectroelectrochemistry is a very suitable tool for such an investigation, since (i) it can help to elucidate reaction pathways and to formulate reaction schemes and (ii) the spectroscopic data on the redox products help considerably to clarify the bonding situation in these species.[10−12]

Investigations of the electrocatalytic CO_2 reduction have mainly been restricted to the halide complexes [Re(X)(CO)$_3$-(α-diimine)] (X = Cl$^-$, Br$^-$; α-diimine = 2,2′-bipyridine, 4,4′-dimethyl-2,2′-bipyridine). Since labilization of the axial halide ligand X upon reduction is of major importance for the complex to act as a catalyst precursor,[11] we have directed our efforts to the study of other suitable candidates for this type of redox reactivity. Replacement of the axial halide ligand X in the complexes [Re(X)(CO)$_3$(α-diimine)] by an alkyl substituent R has a pronounced effect on their photochemical behavior. Whereas the halide species are virtually photostable,[18−23] the

* To whom correspondence should be addressed.

[⊗] Abstract published in *Advance ACS Abstracts,* September 1, 1996.

(1) Chen, P.; Duesing, R.; Graff, D. K.; Meyer, T. *J. Phys. Chem.* **1991**, *95*,
(2) Schanze, K. S.; MacQueen, D. B.; Perkins, T. A.; Cabana, L. A. *Coord. Chem. Rev.* **1993**, *122*, 63.
(3) Stufkens, D. J. *Comments Inorg. Chem.* **1992**, *13*, 359.
(4) Kutal, C.; Corbin, J.; Ferraudi, G. *Organometallics* **1987**, *6*, 553.
(5) Hawecker, J.; Lehn, J. M.; Ziessel, R. *Helv. Chim. Acta* **1986**, *69*, 1990.
(6) Calzaferri, G.; Hadener, K.; Li, J. *J. Photochem. Photobiol., A* **1992**, *64*, 259.
(7) Hawecker, J.; Lehn, J. M.; Ziessel, R. J. *J. Chem. Soc., Chem. Commun.* **1984**, 328.
(8) Sullivan, B. P.; Bolinger, C. M.; Conrad, D.; Vining, W. J.; Meyer, T. J. *J. Chem. Soc., Chem. Commun.* **1985**, 1414.
(9) O'Toole, T. R.; Sullivan, B. P.; Bruce, M. R. M.; Margerum, L. D.; Murray, R. W.; Meyer, T. J. *J. Electroanal. Chem. Interfacial Electrochem.* **1989**, *259*, 217.
(10) Stor, G. J.; Hartl, F.; van Outersterp, J. W. M.; Stufkens, D. J. *Organometallics* **1995**, *14*, 1115.
(11) Johnson, F. P. A.; George, M. W.; Hartl, F.; Turner, J. J. *Organometallics* **1996**, *15*, 3374.
(12) Christensen, P.; Hamnett, A.; Muir, A. V. G.; Timney, J. A. *J. Chem. Soc., Dalton Trans.* **1992**, 1455.
(13) Shu, C.-F.; Wrighton, M. S. Unpublished results, 1988 (see also ref 11).
(14) Sullivan, B. P.; Bruce, M. R.; O'Toole, T. R.; Bolinger, M. R.; Megehee, E.; Thorp, H.; Meyer, T. J. *ACS. Symp. Ser. No.* **1988**, *363*, 52−90.
(15) Cabrera, C. R.; Abruña, H. D. *J. Electroanal. Chem. Interfacial Electrochem.* **1986**, *209*, 101.
(16) Breikss, A. J.; Abruña, H. D. *J. Electroanal. Chem. Interfacial Electrochem.* **1986**, *201*, 347.
(17) Lee, Y. F.; Kirchhoff, J. R.; Berger, R. M.; Gosztola, D. *J. Chem. Soc., Dalton Trans.* **1995**, 3677.
(18) Kalyanasundaram, K. *J. Chem. Soc., Faraday Trans. 2* **1986**, *82*, 2401.
(19) George, M. W.; Johnson, F. P. A.; Westwell, J. R.; Hodges, P. M.; Turner, J. J. *J. Chem. Soc., Dalton Trans.* **1993**, 2977.
(20) Caspar, J. V.; Meyer, T. J. *J. Phys. Chem.* **1983**, *87*, 952.
(21) Balk, R. W.; Stufkens, D. J.; Oskam, A. *J. Chem. Soc., Dalton Trans.* **1981**, 1124.

S0020-1669(96)00094-8 CCC: $12.00

[Re(R)(CO)$_3$(α-diimine)] complexes undergo a homolysis reaction upon irradiation into their metal-to-ligand charge transfer (MLCT) band, resulting in the formation of radicals R$^\bullet$ and [Re(CO)$_3$(α-diimine)]$^\bullet$.[24,25] The efficiency of this photoreaction strongly depends on the α-diimine ligand and the R group used. This striking difference in the photoreactivity has stimulated us to carry out (spectro)electrochemical experiments with the complexes [Re(R)(CO)$_3$(iPr-DAB)] (R = Me, Et, Bz), with the aim of proving whether the cleavage of the Re−R bond occurs also upon their electrochemical reduction.

The formation of the five-coordinate radicals [Re(CO)$_3$(bpy)]$^\bullet$ is one of the crucial steps in the mechanism of the electrocatalytic CO_2 reduction with the complexes [Re(X)(CO)$_3$(bpy)] (X = Cl$^-$, Br$^-$).[9,11,12] An important role in the catalytic mechanism is also played by the six-coordinate radicals [Re(X)(CO)$_3$(bpy)]$^{\bullet-}$ and [Re(L′)(CO)$_3$(bpy)]$^\bullet$ (L′ = RCN, PR$_3$, P(OR)$_3$) as catalyst precursors.[11] Recent (spectro)electrochemical investigation of the reduction pathways of [Re(X)(CO)$_3$(α-diimine)] and [Re(L′)(CO)$_3$(α-diimine)]$^+$ (X = Cl$^-$, Br$^-$, I$^-$, Otf$^-$; L′ = THF, nPrCN, PPh$_3$, P(OMe)$_3$; α-diimine = bpy, iPr-PyCa, dpp, abpy, *N*,*N*′-dapa[26]) has shown[10] that the stability of the Re−L′ or Re−X bond in the six-coordinate radical anions/radicals increases with an increase of π-acceptor ability of the α-diimine ligand, which correlates with its lowest π^* orbital energy. Another important factor is the electron density at the coordinating nitrogen atoms of the reduced α-diimine ligand that determines the amount of additional electron density transferred to the Re−X bond, as was demonstrated for a series of four isomeric bidiazine complexes [Re(X)(CO)$_3$(bdz)]$^{\bullet-}$.[27,28] This electron density might be rather high in the case of [Re(X)(CO)$_3$(α-diimine)]$^{\bullet-}$, where α-diimine is a nonaromatic R′-DAB ligand, *e.g.* with R′ = tBu.[28] As a result, the Re−X bond can split more easily in the latter radical anions than in [Re(X)(CO)$_3$(α-diimine)]$^{\bullet-}$ with an aromatic α-diimine ligand of a π-acceptor ability comparable with that of R′-DAB, *e.g.* 2,2′-bipyrimidine (bpym). We have therefore been interested in the effect of a subtle variation of the R′-DAB properties on the reduction route of [Re(X)(CO)$_3$(R′-DAB)], changing the R′ substituents from alkyls to aryls in order to increase the aromatic character of R′-DAB. In this paper, we describe the results of a (spectro)electrochemical study of the complexes [Re(Br)(CO)$_3$(R′-DAB)] (R′-DAB = iPr, pTol, pAn).

The two-electron pathway of electrocatalytic CO_2 reduction using [Re(X)(CO)$_3$(bpy)] involves the five-coordinate anion [Re(CO)$_3$(bpy)]$^-$.[8,9,11] In sharp contrast to the studies of the radical complexes [Re(X)(CO)$_3$(α-diimine)]$^{\bullet-}$ and [Re(L′)(CO)$_3$(α-diimine)]$^\bullet$, there has been only a limited effort to characterize [Re(CO)$_3$(bpy)]$^-$ and some other [Re(CO)$_3$(α-diimine)]$^-$ anions spectroscopically (IR, UV−vis).[10,12,17] It is therefore not surprising that, owing to the apparent shortage of spectroscopic data, the bonding properties of [Re(CO)$_3$(α-diimine)]$^-$ are only poorly understood. Notably, in a majority of papers, [Re(CO)$_3$(α-diimine)]$^-$ have been considered as d^7 Re^0 species.[12,17] The rather variable CO stretching wavenumbers[10,12] of [Re(CO)$_3$(α-diimine)]$^-$ however indicate that such a simplified description is not acceptable and that the bonding situation in these anions is considerably determined by the character of the α-diimine ligand. Hence, to better understand their bonding properties, we have examined the spectroscopic (IR, UV−vis) data of [Re(CO)$_3$(R′-DAB)]$^-$ and compared them with those of other [Re(CO)$_3$(α-diimine)]$^-$ and related [Mn(CO)$_3$(iPr-DAB)]$^-$ complexes. The result is presented hereinafter in the form of a qualitative MO diagram.

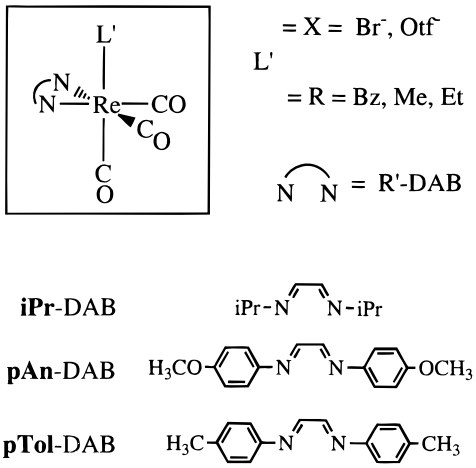

Figure 1. Schematic representation of the molecular structure of the complexes studied and the α-diimine ligands used.

The electrochemical and spectroelectrochemical (IR, UV−vis) data reported in this article were obtained by application of cyclic voltammetry, bulk electrolysis, and electrolysis in optically transparent thin-layer electrolytic (OTTLE) cells at variable temperatures.

The structures of the complexes and the R′-DAB ligands used are schematically depicted in Figure 1.

Experimental Section

Materials and Preparations. The solvents butyronitrile (nPrCN, Fluka), toluene (Aldrich), 1,2-dimethoxyethane (DME, Janssen Chimica), and tetrahydrofuran (THF, Janssen Chimica) were dried on CaH_2 (nPrCN) or Na wire (toluene, DME, THF) and distilled under nitrogen prior to use. The supporting electrolytes Bu_4NPF_6 (Fluka) and Bu_4NBr (Kodak) were dried overnight under vacuum at 353 K before use. PPh_3 (Aldrich) was recrystallized from a diethyl ether solution at 223 K. Ferrocene (Fc, BDH) and Ag^+Otf^- ($Otf^- = CF_3SO_3^-$, Aldrich) were used as received.

The complexes [Re(Br)(CO)$_3$(α-diimine)][29] (α-diimine = iPr-DAB, pAn-DAB, pTol-DAB), [Re(Otf)(CO)$_3$(iPr-DAB)],[10,30] and [Re(R)(CO)$_3$(iPr-DAB)][31] (R = Et, Me, Bz) were synthesized according to literature procedures. [Re(Br)(CO)$_3$(α-diimine)] and [Re(R)(CO)$_3$(iPr-DAB)] were purified by column chromatography over Silica 60 (Merck), activated by heating overnight under vacuum at 433 K, with a gradient elution of *n*-hexane/THF. The purity of the complexes was checked by UV−vis, IR, ^{1}H-NMR, and mass spectroscopy.

The samples for (spectro)electrochemistry were carefully prepared under a nitrogen atmosphere using standard Schlenk techniques. The solutions of the light-sensitive complexes [Re(R)(CO)$_3$(iPr-DAB)] were carefully handled in the dark.

(22) Smothers, W. K.; Wrighton, M. S. *J. Am. Chem. Soc.* **1983**, *105*, 1067.
(23) Worl, L. A.; Duesing, R. P. C.; Della Ciana, L.; Meyer, T. J. *J. Chem. Soc., Dalton Trans.* **1991**, 849.
(24) Rossenaar, B. D.; Kleverlaan, C. J.; Stufkens, D. J.; Oskam, A. *J. Chem. Soc., Chem. Commun.* **1994**, 63.
(25) Lucia, L. A.; Burton, R. D.; Schanze, K. S. *Inorg. Chim. Acta* **1993**, *208*, 103.
(26) Abbreviations used: bpy = 2,2′-bipyridine; dmbpy = 4,4′-Me$_2$bpy; iPr-PyCa = pyridine-2-carbaldehyde *N*-isopropylimine; dpp = 2,3-bis(2-pyridyl)pyrazine; abpy = azo-2,2′-pyridine; *N*,*N*′-dapa = 2,6-diacetylpyridine bis(anil); R′-DAB = *N*,*N*′-di-R′-1,4-diaza-1,3-butadiene (R′ = iPr, pTol, pAn); SOMO = singly occupied molecular orbital.
(27) Kaim, W.; Kramer, H. E. A.; Vogler, C.; Rieker, J. *J. Organomet. Chem.* **1989**, *367*, 107.
(28) Klein, A.; Vogler, C.; Kaim, W. *Organometallics* **1996**, *15*, 236.
(29) Staal, L. H.; Oskam, A.; Vrieze, K. *J. Organomet. Chem.* **1979**, *170*, 235.
(30) Sullivan, B. P.; Meyer, T. J. *J. Chem. Soc., Chem. Commun.* **1984**, 1244.
(31) Rossenaar, B. D.; Kleverlaan, C. J.; van de Ven, M. C. E.; Stufkens, D. J.; Oskam, A.; Goubitz, K.; Fraanje, J. *J. Organomet. Chem.* **1995**, *493*, 153.

Table 1. IR ν(CO) and UV−Vis Data for [Re(X)(CO)$_3$(iPr-DAB)] (X = Br$^-$, Otf$^-$), [Re(L′)(CO)$_3$(iPr-DAB)]$^+$, [Re(R)(CO)$_3$(iPr-DAB)] (R = Me, Et, Bz), and Their Reduction Products in nPrCN (Unless Stated Otherwise)

no.	complex	T, K	ν(CO), cm^{-1}	k_{av}, N m^{-1}	λ_{max}, nm (ϵ_{max}, cm^{-1} M^{-1})
1	[Re(Otf)(CO)$_3$(iPr-DAB)]	293	2035 (s), 1932 (m), 1920 (m)	1556	371
2	[Re(Br)(CO)$_3$(iPr-DAB)]	293	2020 (s), 1921 (m), 1905 (m)	1535	435 (3500)
		193	2020 (s), 1916 (m), 1902 (m)	1530	419
3	[Re(Me)(CO)$_3$(iPr-DAB)]	293	1994 (s), 1888 (m, br)	1495	446 (7150)
4	[Re(Et)(CO)$_3$(iPr-DAB)]	293	1992 (s), 1887 (m, br)	1493	454 (7400)
		193	1991 (s), 1884 (m, br)	1489	442
5	[Re(Bz)(CO)$_3$(iPr-DAB)]	293	1997 (s), 1894 (m, br)	1503	426 (4950), 499 (sh)
6	[Re(nPrCN)(CO)$_3$(iPr-DAB)]$^+$	293	2041 (s), 1943 (s, br)	1577	
		193	2038 (s), 1932 (s, br)	1564	
7	[Re(THF)(CO)$_3$(iPr-DAB)]$^+$	293[a]	2021 (s), 1920 (s), 1899 (s)	1532	
8	[Re(PPh$_3$)(CO)$_3$(iPr-DAB)]$^+$	293	2039 (s), 1957 (s), 1930 (s)	1577	
9	[Re(nPrCN)(CO)$_3$(iPr-DAB)]$^\bullet$	293	2005 (s), 1894 (br)	1507	359, 441, 474 (sh)
		193	2003 (s), 1894 (s), 1879 (s)	1498	
10	[Re(THF)(CO)$_3$(iPr-DAB)]$^\bullet$	293[a]	2007 (s), 1891 (s), 1875 (s)	1497	
11	[Re(PPh$_3$)(CO)$_3$(iPr-DAB)]$^\bullet$	293	2006 (s), 1906 (s), 1877 (s)	1505	346, 450, 500 (sh)
12	[Re(Br)(CO)$_3$(iPr-DAB)]$^{\bullet-}$	293	1990 (s), 1872 (s), 1846 (s)	1464	
		193	1987 (s), 1868 (m), 1851 (m)	1462	
13	[Re(nPrCN)(CO)$_3$(iPr-DAB)]$^-$	293	1988 (s), 1858 (br, s)[b]	1461	
14	[Re(CO)$_3$(iPr-DAB)]$^-$	293	1943 (s), 1828 (vs, br)	1408	440 (7900 ± 100)
		293[a]	1942 (s), 1831 (vs, br)	1410	
		193	1942 (s), 1825 (vs, br)	1404	436
15	[Re(CO)$_3$(iPr-DAB)]$^-\cdots$Me$^\bullet$	293	1955 (s), 1828 (vs, br)	1414	400 (4800)
16	[Re(CO)$_3$(iPr-DAB)]$^-\cdots$Et$^\bullet$	293	1952 (s), 1826 (vs, br)	1411	410 (4950)
		193	1953 (m), 1824 (vs, br)	1409	400
17	[Re(CO)$_3$(iPr-DAB)]$^-\cdots$Bz$^\bullet$	193	1962 (s), 1835 (vs, br)	1425	390

[a] In THF. [b] Obtained from difference IR spectra.

(Spectro)electrochemical Measurements and Instrumentation. IR spectra were recorded on a Bio-Rad FTS-7 FTIR spectrometer (16 scans, resolution of 2 cm^{-1}, thermostated DTGS detector). Electronic absorption spectra were measured on a Perkin-Elmer Lambda 5 UV−vis spectrophotometer, attached to a 3600 data station. A Varian E6 X-band spectrometer with 100 kHz modulation was used to measure ESR spectra. The presented values of the g factor were determined using α,α′-diphenyl-β-picrylhydrazyl (DPPH) as the external standard (g_{DPPH} = 2.0037, H_{DPPH} = 338.6 mT). IR and UV−vis spectroelectrochemical measurements at room temperature were performed in an OTTLE cell,[32] equipped with a Pt-minigrid working electrode (32 wires/cm). For low-temperature IR and UV−vis spectroelectrochemistry, a purpose-made OTTLE cell[33] was used in combination with a home-built, liquid-nitrogen cryostat.[34] A PA4 potentiostat (EKOM) was used to carry out the controlled-potential electrolyses and the cyclic voltammetric measurements. Cyclic voltammetric data were also recorded with a PAR Model 283 potentiostat.

In a typical IR and UV−vis OTTLE measurement, the solution was 0.3 M in the supporting electrolyte and 5×10^{-3}−1×10^{-2} M in the Re complex. For cyclic voltammetry (CV) the concentrations were 0.1 and 10^{-3} M, respectively.

Bulk electrolysis was carried out in a gastight cell that consisted of three electrode compartments separated at the bottom by frits. The compartment of the Pt-flag working electrode (surface of 120 mm^2) was filled with a solution that was 0.3 M in Bu_4NPF_6 and 5×10^{-3} M in the Re complex. The compartments of the Ag-wire pseudoreference and Pt-gauze auxiliary electrodes were filled with 0.3 M electrolyte solution. A cyclic voltammogram of the sample in the electrolysis cell was recorded before starting the electrolysis. The electrolysis was stopped after the cathodic current had dropped below 10 % of its initial value.

Cyclic voltammograms were recorded in nPrCN at 293 and 223 K in a light-protected CV cell with Pt-disk working electrodes of 0.61 and 0.38 mm^2 apparent (electrochemical) surface areas (obtained from the Cottrell equation using $K_4[Fe(CN)_6]$ in aqueous 2.0 M KCl), a Pt-gauze auxiliary electrode, and an Ag-wire pseudoreference electrode. The standard ferrocene/ferrocenium (Fc/Fc$^+$) redox couple[35] served as an internal reference for the determination of the reduction potentials, the electrochemical reversibility of the redox steps, and the number of electrons transferred.

Results

IR and UV−Vis Spectroelectrochemistry. The IR $\tilde{\nu}$(CO) wavenumbers and UV−vis absorption maxima of the complexes under study and their reduction products are collected in Tables 1 and 2, respectively. Table 3 presents the reduction potentials of these compounds. In the following sections the spectroscopic changes upon reduction of the complexes [Re(X)(CO)$_3$(iPr-DAB)] (X = Otf$^-$, Br$^-$), [Re(Br)(CO)$_3$(α-diimine)] (α-diimine = pTol-DAB, pAn-DAB), and [Re(R)(CO)$_3$(iPr-DAB)] (R = Me, Et, Bz) will be discussed separately. The measurements were carried out in nPrCN, unless stated otherwise. Boldface numbers refer to the parent complexes and the products used in the schemes and tables.

In order to discuss the electronic effects in the reduced species, their average C≡O force constants k_{av} were calculated according to eq 1[36] (see Tables 1 and 2).

$$k_{av} = 4.0383 \times 10^{-4} \frac{\sum_i g_i \nu_i^2}{\sum_i g_i} \qquad (1)$$

g_i = degeneracy of ith CO stretching mode of frequency ν_i(cm^{-1})

The lack of information with respect to the exact geometry of the five-coordinate anions [Re(CO)$_3$(R′-DAB)]$^-$ (*vide infra*) prevented the exact determination of all four CO force constants (k_{ax}, k_{eq}, $k_{ax,eq}$, $k_{eq,eq}$) by the empirical method of Timney.[37] Also

(32) Krejčík, M.; Daněk, M.; Hartl, F. *J. Electroanal. Chem. Interfacial Electrochem.* **1991**, *317*, 179.
(33) Hartl, F.; Luyten, H.; Nieuwenhuis, H. A.; Schoemaker, G. *Appl. Spectrosc.* **1994**, *48*, 1522.
(34) Andréa, R. R.; Luyten, H.; Vuurman, M. A.; Stufkens, D. J.; Oskam, A. *Appl. Spectrosc.* **1986**, *40*, 1184.
(35) Gritzner, G.; Kuta, J. *Pure Appl. Chem.* **1984**, *56*, 461.
(36) Braterman, P. S. *Metal Carbonyl Spectra*; Academic Press: London, 1975.
(37) Timney, J. A. *Inorg. Chem.* **1979**, *18*, 2502.

Table 2. IR ν(CO) and UV−Vis Data for [Re(Br)(CO)$_3$(α-diimine)] (α-diimine = pTol-DAB, pAn-DAB) and Their Reduction Products in nPrCN at 293 and 198 K

no.	complex	*T*, K	ν(CO), cm^{-1}	k_{av}, N m^{-1}	λ_{max}, nm (ϵ_{max}, cm^{-1} M^{-1})
18	[Re(Br)(CO)$_3$(pTol-DAB)]	293	2024 (s), 1931 (m), 1909 (m)	1544	
		198	2020 (s), 1909 (s, br)	1530	355 (13 000), 450 (sh)
19	[Re(Br)(CO)$_3$(pAn-DAB)]	293	2024 (s), 1929 (m), 1909 (m)	1543	
		198	2020 (s), 1910 (s, br)	1531	394 (br) (14 400)
20	[Re(Br)(CO)$_3$(pTol-DAB)]$^{\bullet-}$	198	1998 (s), 1886 (s), 1864 (s)	1484	396 (11 200), 618 (2000)
21	[Re(Br)(CO)$_3$(pAn-DAB)]$^{\bullet-}$	198	1997 (s), 1884 (s), 1864 (s)	1482	394 (17 600), 628 (3200)
22	[Re(nPrCN)(CO)$_3$(pTol-DAB)]$^{\bullet}$	293	2014 (s), 1899 (s, br)	1517	
23	[Re(nPrCN)(CO)$_3$(pAn-DAB)]$^{\bullet}$	293	2013 (s), 1900 (s, br)	1517	
24	[Re(nPrCN)(CO)$_3$(pTol-DAB)]$^-$	293	1979[a]		
25	[Re(nPrCN)(CO)$_3$(pAn-DAB)]$^-$	293	1979[a]		
26	[Re(CO)$_3$(pTol-DAB)]$^-$	198	1967 (m), 1858 (s), 1842 (s)	1442	463 (4600 ± 100)
27	[Re(CO)$_3$(pAn-DAB)]$^-$	198	1965 (m), 1857 (s), 1842 (s)	1441	462 (5700 ± 100)

[a] Lower-wavenumber bands obscured by bands of [Re(CO)$_3$(R′-DAB)]$^-$.

Table 3. Reduction Potentials (V *vs* Fc/Fc$^+$) of [Re(Br)(CO)$_3$(R′-DAB)], [Re(L′)(CO)$_3$(R′-DAB)]$^+$ (R′ = iPr, pTol, pAn; L′ = PPh$_3$, nPrCN), and [Re(R)(CO)$_3$(iPr-DAB)] (R = Me, Et, Bz) (10^{-3} M) in 0.1 M Bu$_4$NPF$_6$/nPrCN Solution[b] at υ = 100 mV/s (Pt Disk Electrode)

no.	complex/ligand	$E_{1/2}$	E_p[c]
6	[Re(nPrCN)(CO)$_3$(iPr-DAB)]$^+$ [a]	−1.18	−2.06
		−1.19[c]	−2.07
8	[Re(PPh$_3$)(CO)$_3$(iPr-DAB)]$^+$	−1.10	−2.13
	[Re(nPrCN)(CO)$_3$(pTol-DAB)]$^+$ [a]	−0.80	−1.60
	[Re(nPrCN)(CO)$_3$(pAn-DAB)]$^+$ [a]	−0.85	−1.59
2	[Re(Br)(CO)$_3$(iPr-DAB)]	−1.40	−2.41
		−1.41[c]	−2.44
18	[Re(Br)(CO)$_3$(pTol-DAB)]	−1.05	−1.92
19	[Re(Br)(CO)$_3$(pAn-DAB)]	−1.10	−1.99
3	[Re(Me)(CO)$_3$(iPr-DAB)][d]	−1.74	−2.77
4	[Re(Et)(CO)$_3$(iPr-DAB)][e]	−1.73	−2.77
5	[Re(Bz)(CO)$_3$(iPr-DAB)][f]	−1.74	−2.79
	iPr-DAB	−2.3	
	pTol-DAB	−1.96	
	pAn-DAB	−1.99	

[a] Solution of [Re(Otf)(CO)$_3$(R′-DAB)] in nPrCN. [b] At 293 K, unless stated otherwise. [c] At 223 K. [d] Oxidation found at E_p^a = +0.71 V *vs* Fc/Fc$^+$. [e] Oxidation found at E_p^a = +0.61 V *vs* Fc/Fc$^+$. [f] Oxidation found at E_p^a = +0.27 V *vs* Fc/Fc$^+$.

the Cotton−Kraihanzel energy-factored force field method[38−40] could not be used, since the frequencies of the ^{13}CO-enriched positional isotopomers are not known.

Lower k_{av} values of the reduction products imply an increase of the Re→CO π-back-bonding which in turn reflects an increase of electron density at the metal center. The force constants k_{av} may serve, therefore, as good indicators of the changing basicity of the α-diimine ligands within the redox series studied.

[Re(X)(CO)$_3$(iPr-DAB)] (X = Otf$^-$, Br$^-$). The complex [Re(Otf)(CO)$_3$(iPr-DAB)] (**1**) remained thermally stable in nPrCN at 293 K for more than 30 min. IR spectra collected during this time interval did not show any formation of the cation [Re(nPrCN)(CO)$_3$(iPr-DAB)]$^+$ (**6**). In remarkable contrast to this behavior, rapid substitution of the weakly bound Otf ligand by nPrCN was monitored by real-time screen-display FT-IR upon reducing **1** within the IR OTTLE cell at a potential which only corresponded to the onset of the cathodic peak of **1**. This observation points to a catalytic nature of the reaction. Identical electrode-mediated substitution reactions were reported, together with some details of the reaction mechanism, for the corresponding complexes [Re(Otf)(CO)$_3$(α-diimine)] (α-diimine = bpy, iPr-PyCa, abpy).[10] Complex **1** underwent this electrode-catalyzed reaction also in THF, as could be concluded from the apparent similarity between the ν(CO) frequencies of [Re(THF)(CO)$_3$(α-diimine)]$^+$ [10] and the product [Re(THF)(CO)$_3$(iPr-DAB)]$^+$ (**7**) (see Table 1).

One-electron reduction of cation **6** only led to the formation of [Re(nPrCN)(CO)$_3$(iPr-DAB)]$^{\bullet}$ (**9**) (Table 1). No dimeric species [Re$_2$(CO)$_6$(iPr-DAB)$_2$] was produced. This result testifies to an inherent stability of **9**. The IR OTTLE results also rule out the occurrence of a C−C coupling reaction between two five-coordinate radicals [Re(CO)$_3$(iPr-DAB)]$^{\bullet}$, as was observed[10] for [Re(CO)$_3$(iPr-PyCa)]$^{\bullet}$ with one reactive C=N imino bond.

The reduction of **1** in nPrCN led to the replacement of its MLCT absorption band at 371 nm by new bands of **9** at 359, 441, and 474 (sh) nm. No absorption was observed in the red spectroscopic region which would otherwise indicate the formation of [Re$_2$(CO)$_6$(iPr-DAB)$_2$]. For, an intense low-lying MLCT band is a characteristic feature of related metal−metal-bonded dimers, *e.g.* [Re$_2$(CO)$_6$(bpy)$_2$],[16,41] [Ru$_2$(Me)$_2$(CO)$_4$(iPr-DAB)$_2$],[33,42,43] and [Mn$_2$(CO)$_6$(iPr-DAB)$_2$].[44,45] This result again proves that the dimer [Re$_2$(CO)$_6$(iPr-DAB)$_2$] was not formed, even in low concentration.

In order to establish whether the dimerization of [Re(CO)$_3$(iPr-DAB)]$^{\bullet}$ was only prevented due to the strong coordinating ability of the nPrCN solvent,[10] the reduction of **1** was also carried out in THF. Also in this case the one-electron reduction produced exclusively the radical [Re(THF)(CO)$_3$(iPr-DAB)]$^{\bullet}$ (**10**) (Table 1).

Subsequent reduction of **9** resulted in product **14** with $\tilde{\nu}$(CO) wavenumbers at 1943 (s) and 1828 (vs, br) cm^{-1} and an intense absorption band at 440 nm. These data closely correspond to those reported by Stor *et al.*[10] for [Re(CO)$_3$(bpy)]$^-$ and [Re(CO)$_3$(iPr-PyCa)]$^-$. The product **14** is, therefore, assigned to [Re(CO)$_3$(iPr-DAB)]$^-$. Apart from this five-coordinate anion, a very small amount of six-coordinate [Re(nPrCN)(CO)$_3$(iPr-DAB)]$^-$ (**13**) was also formed. The assignment of **13** was based on the similarity of its $\tilde{\nu}$(CO) wavenumbers (Table 1) to those recently reported for the corresponding anions [Re(nPrCN)-

(38) Turner, J. J.; Grevels, F. W.; Howdle, S. M.; Jacke, J.; Haward, M. T.; Klotzbücher, W. E. *J. Am. Chem. Soc.* **1991**, *113*, 8347.
(39) Kraihanzel, C. S.; Cotton, F. A. *Inorg. Chem.* **1963**, *2*, 533.
(40) Cotton, F. A.; Kraihanzel, C. S. *J. Am. Chem. Soc.* **1962**, *84*, 4432.
(41) Servaas, P. C.; Stor, G. J.; Stufkens, D. J.; Oskam, A. *Inorg. Chim. Acta* **1990**, *178*, 185.
(42) tom Dieck, H.; Rohde, W.; Behrens, U. *Z. Naturforsch.* **1989**, *44B*, 158.
(43) Nieuwenhuis, H. A.; van Loon, A.; Moraal, M. A.; Stufkens, D. J.; Oskam, A.; Goubitz, K. *J. Organomet. Chem.* **1995**, *492*, 165.
(44) Rossenaar, B. D.; Hartl, F.; Stufkens, D. J.; Amatore, C.; Maisonhaute, E.; Verpeaux, J.-N. *Organometallics*, submitted for publication.
(45) Rossenaar, B. D.; Stufkens, D. J.; Oskam, A.; Fraanje, J.; Goubitz, K. *Inorg. Chim. Acta* **1996**, *247*, 215.

$(CO)_3$(iPr-PyCa)]$^-$ [10] and [Re(nPrCN)$(CO)_3$(bpy)]$^-$.[11,46] One-electron reduction of **10** also led to the formation of **14**.

The IR spectral changes accompanying the reduction of **6** are depicted in Figure 2 (Supporting Information).

The electrode-catalyzed/electron transfer chain (ETC) substitution[10] of the Otf ligand in **1** also took place in the presence of a 40-fold excess of PPh_3 and afforded the cation [Re(PPh_3)-$(CO)_3$(iPr-DAB)]$^+$ (**8**). This complex could be reduced with one electron to give the stable radical [Re(PPh_3)$(CO)_3$(iPr-DAB)]$^\bullet$ (**11**) and, in a second step, the five-coordinate anion **14**. Both steps were fully chemically reversible since cation **8** could be completely recovered by successive reoxidation of **14** and **11**.

One-electron reduction of [Re(Br)$(CO)_3$(iPr-DAB)] (**2**) in nPrCN at 293 K led initially to the product **12**. This species could, however, only be seen in low concentration, since it partly underwent a thermal reaction to give the solvento radical **9**. The IR $\tilde{\nu}$(CO) wavenumbers of **12** (Table 1) are very close to those of the corresponding [Re(Br)$(CO)_3$(α-diimine)]$^{\bullet-}$ complexes (α-diimine = bpy, iPr-PyCa)[10] and are, therefore, assigned to [Re(Br)$(CO)_3$(iPr-DAB)]$^{\bullet-}$. The position of the equilibrium between [Re(Br)$(CO)_3$(iPr-DAB)]$^{\bullet-}$ (**12**) and [Re-(nPrCN)$(CO)_3$(iPr-DAB)]$^\bullet$ (**9**) was estimated from IR spectroelectrochemical data by comparing the absorbances of the highest frequency ν(CO) band of both species (Table 1) after the exhaustive reduction of the parent [Re(Br)$(CO)_3$(iPr-DAB)] (**2**) had taken place. The extinction coefficients of the ν(CO) bands of both radicals were assumed to be similar. The ratio **12**/**9** was 0.22. Performing the IR OTTLE experiment at 198 K was not sufficient to stabilize the radical anion **12**, although the ratio **12**/**9** increased to 0.73. An even better result was obtained at 198 K with 3×10^{-1} M Br^- ions in the solution. The equilibrium between **12** and **9** was then shifted considerably toward **12** (ratio **12**/**9** = 1.63).

The existence of the equilibrium between the radicals **12** and **9** was directly proved by the subsequent reduction of **9** to give the anion [Re$(CO)_3$(iPr-DAB)]$^-$ (**14**). This reduction was immediately accompanied by the parallel disappearance of **12**, despite the fact that the latter radical is reduced 350 mV more negatively with respect to the reduction potential of **9** (see Table 3).

In the presence of an 80-fold excess of PPh_3 at 293 K, **2** was reduced to give directly radical **11**. No trace of **12** was detected in the solution, which confirms that the Br^- ligand in [Re(Br)-$(CO)_3$(α-diimine)]$^{\bullet-}$ is in general[10] more easily substituted by PPh_3 than by nPrCN. Not only did reoxidation of **11** formed from **2** produce the cationic complex **8**, but also 85% of **2** was recovered by a thermal reaction of **8** with Br^- still present in the thin solution layer.

The reduction routes of the complexes **1** and **2** are summarized in Scheme 1.

[Re(Br)$(CO)_3$(R′-DAB)] (R′ = pTol, pAn). One-electron reduction of [Re(Br)$(CO)_3$(R′-DAB)] (**18**, **19**) in nPrCN led in both cases to the formation of [Re(Br)$(CO)_3$(R′-DAB)]$^{\bullet-}$ (**20**, **21**), followed by the substitution of Br^- by a solvent molecule to give the radicals [Re(nPrCN)$(CO)_3$(R′-DAB)]$^\bullet$ (**22**, **23**). However, the yield of the latter solvento radicals differed substantially from that of **9** formed by reduction of **2**. At 293 K, the [Re(Br)$(CO)_3$(R′-DAB)]$^{\bullet-}$/[Re(nPrCN)$(CO)_3$(R′-DAB)]$^\bullet$ ratios were 0.81 for R′ = pTol and 1 for R′ = pAn. Both values are apparently much higher than 0.22 for R′ = iPr (*vide supra*). Hence, the halide coordination in [Re(Br)$(CO)_3$(R′-DAB)]$^{\bullet-}$ is significantly stabilized by the introduction of an electron-withdrawing R′ group into the R′-DAB ligand.

Scheme 1

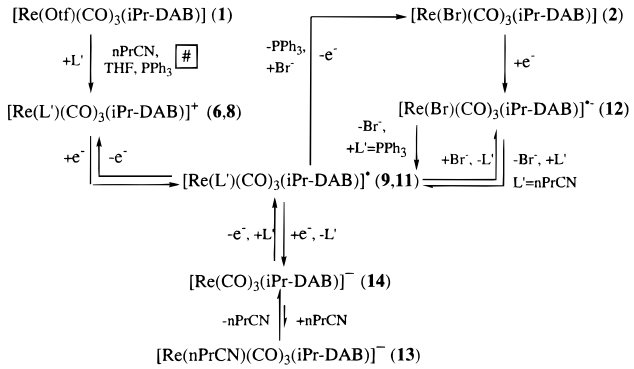

electrode-catalyzed substitution of Otf by L'

In order to stabilize the radical anions **20** and **21**, Bu_4NBr was used as electrolyte instead of Bu_4NPF_6 and the temperature was lowered to 198 K. The solvento radicals **22** and **23** were not observed in this case. The radical anions **20** and **21** were further reduced to give the five-coordinate anions [Re$(CO)_3$-(R′-DAB)]$^-$ (**26** and **27**, respectively). In addition, small amounts of the six-coordinate anions [Re(nPrCN)$(CO)_3$(R′-DAB)]$^-$ (**24** and **25**, respectively) were observed.

The successive reduction steps of [Re(Br)$(CO)_3$(R′-DAB)] at 198 K were also monitored in the UV−vis region. Complexes **18** and **19** possess very strong intraligand (IL) $\pi \rightarrow \pi_1^*$ transitions in the near-UV region, together with MLCT transitions which manifest themselves as shoulders at the low-energy sides of the IL bands[21] (Table 2, Figure 3 (Supporting Information)). In the UV−vis spectra of radicals **20** and **21** the strong IL $\pi \rightarrow \pi_1^*$ band shifted to 396 and 394 nm, respectively. At the same time, less intense broad bands were present at 618 nm for **20** and 628 nm for **21**. Subsequent reduction of **20** and **21** resulted in the appearance of single bands in the visible region at 463 and 462 nm, assigned to anions **26** and **27**, respectively. The UV−vis spectra of **18**, **20**, and **26** are presented in Figure 3.

In order to assign the lowest absorption band in the UV−vis spectra of the radical anions **20** (see Figure 3) and **21**, we recorded the UV−vis spectra of the singly reduced free ligands [R′-DAB]$^{\bullet-}$. One-electron reduction of R′-DAB (Table 3) led to the disappearance of their intense $\pi \rightarrow \pi_1^*$ (HOMO → LUMO) IL absorption bands at 353 (R′ = pTol) and 380 (R′ = pAn) nm. New bands of [R′-DAB]$^{\bullet-}$ appeared at 440, 660 (R′ = pTol) and 440, 658 (R′ = pAn) nm. The higher energy band in the UV−vis spectra of [R′-DAB]$^{\bullet-}$ probably belongs to the $\pi \rightarrow \pi_1^*$ (HOMO → SOMO[26]) transition which is thus shifted to lower energies with respect to $\pi \rightarrow \pi_1^*$ of neutral R′-DAB. The lowest-energy absorption band of [R′-DAB]$^{\bullet-}$ probably has its origin in a $\pi_1^* \rightarrow \pi_2^*$ (IL) electronic transition, *i.e.* in electron transfer from the π_1^* SOMO to a higher-lying empty π_2^* orbital which might mainly reside on the R′ substituents. These bands are very similar in position, intensity, and shape to the lowest-energy absorption bands of the radical complexes **20** and **21** (Table 2, Figure 3), which are therefore also assigned to the $\pi_1^* \rightarrow \pi_2^*$ IL transition, largely localized on the aromatic [R′-DAB]$^{\bullet-}$ ligand.

The electrochemical reduction of complexes **18** and **19** is summarized in Scheme 2.

[Re(R)$(CO)_3$(iPr-DAB)] (R = Me, Et, Bz). Changing the axial donor ligand from Br to R (R = Me, Et, Bz) significantly influenced the redox behavior of the complexes. Reduction of

(46) van Outersterp, J. W. M.; Hartl, F.; Stufkens, D. J. *Organometallics* **1995**, *14*, 3303.

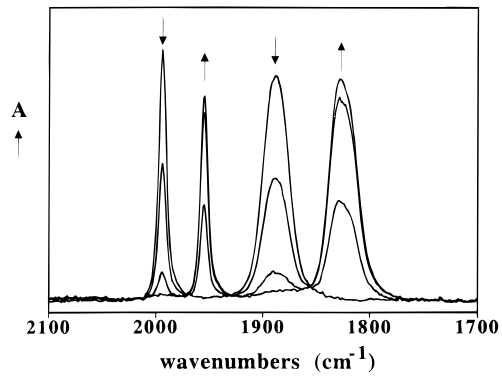

Figure 4. IR spectral changes in the carbonyl stretching region during the reduction of [Re(Me)(CO)$_3$(iPr-DAB)] (**3**) at room temperature in nPrCN.

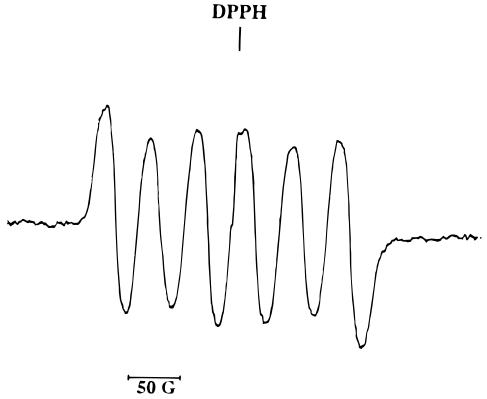

Figure 5. ESR spectrum of **16** generated by bulk electrolysis of **4** in THF at room temperature.

Scheme 2

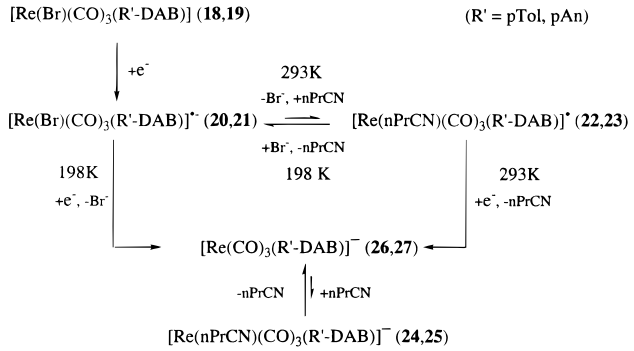

[Re(Me)(CO)$_3$(iPr-DAB)] (**3**) at 293 K led directly to a single product (**15**) with ν(CO) bands at 1955 (s) and 1828 (vs, br) cm^{-1} (see Figure 4). A comparable product (**16**) was formed upon reduction of the Et derivative (**4**) (Table 1). These $\tilde{\nu}$(CO) wavenumbers are clearly too small to belong to radical-type products like **9**−**12**, but they are very similar to those of the five-coordinate anion **14** (Table 1). However, there is an apparent difference in the position of the highest-frequency ν(CO) band, which documents that the products **15** and **16** differ from **14**. This was also revealed by the UV−vis spectra of **15** and **16**, which exhibit the lowest-energy absorption bands at 400 and 410 nm, respectively. Both bands are thus shifted to higher energy with respect to the visible absorption band of anion **14**; besides, their ϵ_{max} values are significantly smaller (Table 1).

Upon reduction of **4** at 293 K, a minor product with ν(CO) bands at 1984 and *ca.* 1860 cm^{-1} was also observed. This is probably a product of a slow secondary reaction of **16**, since its concentration slowly increased with decreasing concentration of **16** and reduction of **4** at 193 K only resulted in the formation of **16**.

Reoxidation of **15** and **16** at 293 K led to the nearly quantitative recovery of the parent complexes **3** and **4**, respectively. A minor yet unidentified species with ν(CO) frequencies at 1971 and *ca.* 1840 (br) cm^{-1} was observed upon reoxidation of **15**. Reoxidation of **16** at 193 K resulted in the complete regeneration of the starting material.

The reduction of **3** was also carried out in the presence of a 60-fold excess of PPh_3. Importantly, no product other than **15** was observed, in sharp contrast to the reduction of **2** under identical conditions that only gives the PPh_3-substituted radical **11**.

In order to characterize the product **16**, bulk electrolysis of 5 × 10^{-3} M **4** in THF was carried out. After 1 h electrolysis that resulted in 90% conversion of the parent complex, no carbonyl complexes other than **4** and **16** were detected in the solution by IR spectroscopy. Allowing oxygen to diffuse slowly into the solution resulted in the smooth reoxidation of **16** into **4**. Figure 5 presents the ESR spectrum of reduced **16** recorded at 293 K. The ESR spectrum was found at $g = 2.0051$ as a sextet due to the hyperfine splitting of the two relevant rhenium isotopes ^{185}Re ($I = {}^5/_2$, 37.4% natural abundance) and ^{187}Re ($I = {}^5/_2$, 62.6%): $a_{Re} = 48.7$ G. It is noteworthy that this splitting constant is larger than those of the five-coordinate tBu-DAB localized radical [Re(CO)$_3$(tBu-DAB)]• (a_{Re} = 35.6 G in toluene)[47] and related six-coordinate radical complexes [Re(Cl)(CO)$_3$(tBu-DAB)]•− (a_{Re} = 19 G)[28] and [Re(L′)(CO)$_3$(tBu-DAB)]• (L′ = CH$_3$CN, a_{Re} = 37.2 G; L′ = PPh_3, a_{Re} = 40.7 G).[28] Unfortunately, the broad lines of the sextet obscured iPr-DAB and Et hyperfine splitting.

The electrochemical reduction of [Re(Bz)(CO)$_3$(iPr-DAB)] (**5**) showed a more complicated pattern, since it resulted in a mixture of at least five products. Two of them could be identified as the radical **9** and the five-coordinate anion **14** (see Table 1). Besides these species, several unidentified products with ν(CO) bands at 1993 and ∼1880 cm^{-1} (**A**), 1979 and ∼1864 cm^{-1} (**B**), and 1970 and ∼1838 cm^{-1} (**C**) were present in the reduced solution. On the contrary, reduction of **5** at 198 K gave, similar to the reduction of **4** at the same temperature, only the single product **17** with ν(CO) bands at 1962(s) and 1835 (vs, br) cm^{-1}. These wavenumbers closely resemble those of **15** and **16** (Table 1). Hence, **17** is proposed to have a comparable structure. Regardless of the low temperature, this product possessed a limited stability and partly decomposed within 15 min to the five-coordinate anion **14**.

Cyclic Voltammetry (CV). The cyclic voltammograms of all complexes [Re(X)(CO)$_3$(R′-DAB)] (X = Otf$^-$, Br$^-$) and [Re(R)(CO)$_3$(iPr-DAB)] (R = Me, Et, Bz) under study were recorded in nPrCN at room temperature and at 223 K. The corresponding reduction potentials are collected in Table 3. The electrochemical reversibility of the reduction steps was determined (i) by comparison of ΔE_p of the sample with that of the standard Fc/Fc$^+$ couple under identical experimental conditions and (ii) from the E_p^c *vs* log υ dependence in the range of 20 mV/s ≤ υ ≤ 2 V/s. In the latter case, E_p^c remained constant for electrochemically and chemically reversible cathodic processes or shifted by 30 mV per 10-fold increase in υ for electrochemically reversible but chemically irreversible steps (an $E_{rev}C$ mechanism; *vide infra*).

Ferrocene also served as an internal standard for the determination of the number of electrons (n) transferred in the

(47) Andréa, R. R.; de Lange, W. G. J.; van der Graaf, T.; Rijkhoff, M.; Stufkens, D. J.; Oskam, A. *Organometallics* **1988**, *7*, 1100.

controversial reduction of [Re(R)(CO)$_3$(iPr-DAB)] (*vide supra*). For [Re(Br)(CO)$_3$(iPr-DAB)] (**2**), where $n = 1$ was already known from the IR OTTLE experiments, the diffusion coefficient was calculated at 298 K according to eq 2,[48] where A is

$$I_p^c = 2.69 \times 10^5 n^{3/2} A D^{1/2} \upsilon^{1/2} C \qquad (2)$$

the apparent surface area of the Pt disk electrode and C is the bulk concentration of the complex. The result is practically identical with that obtained from a comparison with the calculated value of D_{Fc} in nPrCN (1.45×10^{-5} cm^2 s^{-1}) using the reported value of D_{Fc} in acetonitrile[49] and Walden's rule.[50]

The cyclic voltammogram of [Re(Otf)(CO)$_3$(iPr-DAB)] (**1**) (Figure 6 (Supporting Information)) in nPrCN obviously represents the reduction of electrocatalytically produced [Re(nPrCN)(CO)$_3$(iPr-DAB)]$^+$ (**6**), as was demonstrated by the IR OTTLE experiments outlined above. The electrochemically and chemically reversible ($\Delta E_p = 65$ mV *vs* 65 mV for Fc/Fc$^+$ at $\upsilon = 100$ mV/s; $I_p^a/I_p^c = 1$) one-electron reduction of **6** to **9** was found at -1.18 V *vs* Fc/Fc$^+$. Figure 6 reveals that the subsequent reduction of **9** at $E_p^c = -2.06$ V to give the five-coordinate anion **14**, the major product observed with IR spectroelectrochemistry (*vide supra*), is electrochemically quasireversible, obviously as a result of the dissociation of nPrCN.

IR OTTLE experiments witnessed the existence of an equilibrium between the radical anions [Re(Br)(CO)$_3$(R′-DAB)]$^{\bullet-}$ and the solvent-substituted radicals [Re(nPrCN)(CO)$_3$(R′-DAB)]$^\bullet$ formed upon reduction of [Re(Br)(CO)$_3$(R′-DAB)], whose position significantly depended on the R′-DAB ligand used. This was also reflected in the cyclic voltammetric response of [Re(Br)(CO)$_3$(R′-DAB)]. For R′ = pTol (**18**) and pAn (**19**), the one-electron reductions of the parent complexes at 293 K were both electrochemically and chemically reversible. No apparent anodic peaks due to reoxidation of the solvento radicals **22** and **23** (see Table 3) were observed after switching the scan direction beyond the cathodic peaks of **18** and **19**. The radical anions **20** and **21** are thus stable on the CV time scale ($\upsilon \geq 50$ mV/s).

For R′ = iPr (**2**), the first reduction to **12** at 293 K was electrochemically reversible but chemically irreversible ($I_p^a/I_p^c = 0.76$ at $\upsilon = 100$ mV/s, $D_2 = 1.35 \times 10^{-5}$ cm^2 s^{-1}) (see Figure 7a). Scan reversal after passing the cathodic peak of **2** revealed the presence of a new redox couple at $E_{1/2} = -1.18$ V *vs* Fc/Fc$^+$. The anodic process can be assigned to the reoxidation of the solvento radical [Re(nPrCN)(CO)$_3$(iPr-DAB)]$^\bullet$ (**9**) to **6**, in agreement with the cyclic voltammogram of **6** (see Figure 6). Lowering the temperature to 223 K resulted in the increase of the peak-current ratio I_p^a/I_p^c of the couple **12**/**2** to 0.92 (see Figure 7b).

The cyclic voltammograms of all [Re(Br)(CO)$_3$(R′-DAB)] complexes showed a second, more negative, cathodic process which was both electrochemically and chemically irreversible ($I_p^a/I_p^c < 1$ at $\upsilon = 100$ mV/s). It corresponds to the reduction of **12**, **20**, or **21** (Table 3) to the dianions [Re(Br)(CO)$_3$(R′-DAB)]$^{2-}$. The observed irreversibility apparently has its origin in rapid dissociation of Br$^-$ from the dianionic species to give **14**, **26**, and **27**, respectively.

In the cyclic voltammogram of **2** at 293 K, a third cathodic peak (marked with ▼ in Figure 7a) was observed at a more positive potential as compared with the voltammogram for the reduction of **12** (Table 3). This peak belongs to the reduction

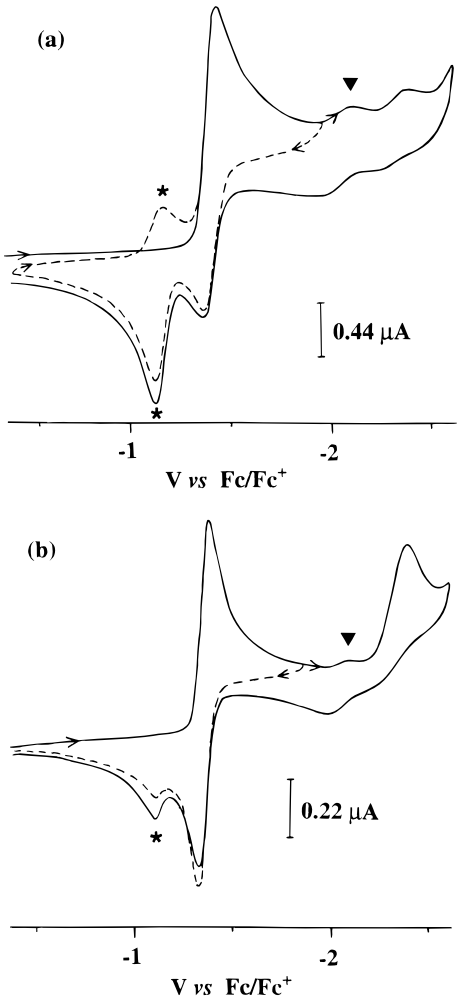

Figure 7. Cyclic voltammograms of 1.2×10^{-3} M [Re(Br)(CO)$_3$(iPr-DAB)] (**2**) in nPrCN at (a) room temperature and (b) 223 K. The asterisk denotes the redox couple [Re(nPrCN)(CO)$_3$(iPr-DAB)]$^{+/\bullet}$ (**6**/**9**). ▼ denotes the reduction of [Re(nPrCN)(CO)$_3$(iPr-DAB)]$^\bullet$ (**9**). − − − = scan reversal *prior* to the reduction of **9** and **12**. Conditions: 8×10^{-4} M solution in nPrCN in the presence of 10^{-1} M Bu_4NPF_6, Pt disk electrode (apparent surface area 0.38 mm^2), $\upsilon = 100$ mV/s, referenced against Fc/Fc$^+$.

of radical **9** present in the solution due to partial dissociation of Br$^-$ from **12**. In accordance with the IR OTTLE results, the peak current ratio E_p^c(**9**)/E_p^c(**12**) decreased upon lowering the temperature to 223 K (Figure 7b).

The cyclic voltammograms of the alkyl complexes [Re(Me)(CO)$_3$(iPr-DAB)] (**3**) and [Re(Et)(CO)$_3$(iPr-DAB)] (**4**) showed one-electron reduction steps at -1.74 and -1.73 V, respectively, which were both chemically and electrochemically reversible (see Figure 8a in the Supporting Information). The calculated diffusion coefficient of (**4**) (using $n = 1$) is $D_4 = 1.22 \times 10^{-5}$ cm^2 s^{-1}, *i.e.* comparable with D_2 (*vide supra*). The chemical reversibility of the reduction fully corresponds with the stability of the products **15** and **16** respectively, as was proved on the time scale of minutes by the spectroelectrochemical measurements. Moreover, it was also reflected in the cyclic voltammogram of the radical anion **16** produced *via* bulk electrolysis of **4**, which was identical with the cyclic voltammogram of **4** recorded *prior* to the electrolysis.

The cyclic voltammogram of [Re(Bz)(CO)$_3$(iPr-DAB)] (**5**) was more complex (see Figure 8b in the Supporting Information). Also in this case, one-electron reduction was observed at $E_p^c = -1.74$ V, which was electrochemically reversible but chemically irreversible ($I_p^a/I_p^c = 0.66$ at 100 mV/s). Additional

(48) Bard, A. J.; Faulkner, L. R. *Electrochemical Methods; Fundamentals and Applications*; John Wiley & Sons: New York, 1980; p 218.
(49) Scholl, H.; Sochaj, K. *Electrochim. Acta* **1991**, *36*, 689.
(50) Walden, P.; Ulich, H.; Busch, G. *Z. Phys. Chem.* **1926**, *123*, 429.

peaks appeared at −1.30 and −1.22 V upon the reverse anodic sweep. The latter peak obviously corresponds to the redox couple **6**/**9** (Figure 8b, Table 3). This result agrees with those of the IR OTTLE experiments at 293 K, where decomposition of the initially formed radical anion **17** was observed. The irreversible anodic process at −1.30 V remained unassigned.

All three radical anions **15**−**17** are further irreversibly reduced at $E_p^c \sim -2.8$ V. The reduction occurred close to the negative limit of the potential window available and was therefore not studied in detail.

Discussion

(Spectro)electrochemical studies of the complexes [Re(Br)(CO)$_3$(α-diimine)] (α-diimine[26] = bpy, iPr-PyCa, dpp, *N*,*N*′-dapa, bpym, abpy)[10,46] demonstrated that the higher the π^* LUMO of the α-diimine in the order abpy < bpym < *N*,*N*′-dapa ∼ dpp < iPr-PyCa < bpy, the more reactive was the one-electron reduction product toward the cleavage of the Re−Br bond. In this respect, the complex [Re(Br)(CO)$_3$(iPr-DAB)] under study may be placed within this series between [Re(Br)(CO)$_3$(dpp)] and [Re(Br)(CO)$_3$(bpym)]. The potentials of the one-electron reduction of these complexes were found at −1.55 and −1.42 V *vs* Fc/Fc$^+$ in THF and DMF, respectively, *i.e.* comparable to the reduction potential of [Re(Br)(CO)$_3$(iPr-DAB)] (see Table 3). In addition, the $\tilde{\nu}$(CO) wavenumbers of the radical anion [Re(Br)(CO)$_3$(dpp)]$^{\bullet-}$ and the radical [Re(THF)(CO)$_3$(dpp)]$^\bullet$ are very similar[10] to those found for the corresponding iPr-DAB complexes (Table 1). In view of these data, it is therefore not surprising that the stability of the reduced species [Re(Br)(CO)$_3$(iPr-DAB)]$^{\bullet-}$ toward the cleavage of the Re−Br bond is comparable[10] to that of [Re(Br)(CO)$_3$(dpp)]$^{\bullet-}$, which also underwent a slow, albeit complete, dissociation of the Br$^-$ ligand to give [Re(THF)(CO)$_3$(dpp)]$^\bullet$.

Variation of the R′ substituents on the DAB ligand has a profound effect on the reactivity of [Re(Br)(CO)$_3$(R′-DAB)]$^{\bullet-}$. Whereas the equilibrium between [Re(Br)(CO)$_3$(iPr-DAB)]$^{\bullet-}$ (**12**) and [Re(nPrCN)(CO)$_3$(iPr-DAB)]$^\bullet$ (**9**) was in favor of **9**, it was significantly shifted toward [Re(Br)(CO)$_3$(R′-DAB)]$^{\bullet-}$ (**20**, **21**) for R′ = pTol, pAn. This difference is attributed to a stabilization of the π^*(R′-DAB) LUMO when iPr is replaced by an electron-withdrawing aromatic group. This was also reflected in the shift of the reduction potential of [Re(Br)(CO)$_3$(R′-DAB)] to more positive values by *ca.* 300 mV when iPr was replaced by pTol or pAn. Thus, the presence of aromatic R′ strongly reduces the electron density on the Re(R′-DAB) chelate ring in [Re(Br)(CO)$_3$(R′-DAB)]$^{\bullet-}$ and considerably stabilizes the radical anion toward release of the halide.

This loss of halide will be caused by a σ- or π-antibonding interaction with the p_σ or p_π orbitals of the halide. The σ interaction may occur by mixing of the π^* DAB orbital of the radical anion with the d_{z^2} and p_z orbitals of the metal, which are σ-antibonding with respect to the halide. The antibonding π interaction takes place between the π^* DAB orbital and a p_π orbital of the halide. Which of these two interactions is primarily responsible for release of the halide is not directly clear. It is the subject of density functional theory calculations, the results of which will be published separately.

However, independent of the type of interaction, the extent of both the σ and π mixing will depend on the electron density in the SOMO[26] at the coordinating nitrogen atoms. This is *e.g.* demonstrated by the large difference in stability between the radical anions [Re(Br)(CO)$_3$(R′-DAB)]$^{\bullet-}$ and [Re(Br)(CO)$_3$(bpym)]$^{\bullet-}$. The former radical anions lose the halide more easily, although they are generated at a less negative potential.[28,46,51] The lower stability of the [Re(Br)(CO)$_3$(R′-DAB)]$^{\bullet-}$ radical anions, in particular for R′ = iPr, is due to the fact that the [R′-DAB]$^{\bullet-}$ ligands have the extra electron density largely localized on the nitrogen atoms, whereas it is extensively delocalized over the ligand in the case of the aromatic [bpym]$^{\bullet-}$.

The unpaired electron in [Re(Br)(CO)$_3$(R′-DAB)]$^{\bullet-}$ (R′ = pTol, pAn) still remains, however, mainly localized on the R′-DAB ligand, as indicated by the close resemblance between the IL transitions in the UV−vis spectra of [Re(Br)(CO)$_3$(R′-DAB)]$^{\bullet-}$ and the reduced ligands [R′-DAB]$^{\bullet-}$.

Substitution of the axial Br$^-$ ligand by an alkyl group R caused a negative shift of the reduction potentials of the [Re(R)(CO)$_3$(iPr-DAB)] complexes by 340 mV compared to that of [Re(Br)(CO)$_3$(iPr-DAB)]. This potential difference can be attributed to strong σ-donating properties of the R ligands, as also revealed by the $\tilde{\nu}$(CO) wavenumbers (and k_{av}) of the parent species. Thus, k_{av} of [Re(Br)(CO)$_3$(iPr-DAB)] is larger by 30−40 N m^{-1} than the value of the [Re(R)(CO)$_3$(iPr-DAB)] complexes (Table 1).

The one-electron reduction of [Re(R)(CO)$_3$(iPr-DAB)] led to the formation of the products **15**−**17** with $\tilde{\nu}$(CO) wavenumbers and UV−vis absorption maxima close to those of the anion [Re(CO)$_3$(iPr-DAB)]$^-$ (**14**). According to these experimental data, the species **15**−**17** are expected to be structurally and electronically comparable with the anion **14**. Cyclic voltammetry revealed, however, that these anion-like products are formed already in a one-electron reduction step, indicating that the R ligand behaves upon the reduction of the parent complexes as a radical R$^\bullet$. This behavior is in sharp contrast with the electrochemical generation of [Re(Br)(CO)$_3$(iPr-DAB)]$^{\bullet-}$, which is followed by the dissociation of the anion Br$^-$. The apparent electrochemical and chemical reversibility of the reduction of [Re(R)(CO)$_3$(iPr-DAB)], together with an R-dependent shift of the $\tilde{\nu}$(CO) wavenumbers of **15**−**17** to larger values with respect to **14**, implies that the R$^\bullet$ radical still interacts with the metal center, hence preserving its intact six-coordinate geometry. On the contrary, the dissociation of Br$^-$ from [Re(Br)(CO)$_3$(R′-DAB)]$^{2-}$ (R′ = iPr, pTol, pAn) to form five-coordinate [Re(CO)$_3$(R′-DAB)]$^-$ makes the one-electron reduction of [Re(Br)(CO)$_3$(R′-DAB)]$^{\bullet-}$ chemically irreversible (see Figure 7b). The same applies for the one-electron reduction of [Re(nPrCN)(CO)$_3$(iPr-DAB)]$^\bullet$, which is electrochemically quasireversible (see Figure 6) due to a dynamic equilibrium between the anionic products **14** and **13** (see Scheme 1). In full agreement with the CV data, the radical character of the products **15**−**17** has been confirmed unambiguously by the recorded ESR spectrum of **16** (see Figure 5).

Combination of all the spectroscopic and electrochemical results led us to the conclusion that complexes **15**−**17** can best be formulated as {[Re(CO)$_3$(iPr-DAB)]$^-$···R$^\bullet$}. Recently, Wissing *et al.*[52] reported that the radical anionic [Zn(R)$_2$(R′-DAB)]$^-$K$^+$ (R = Me, CH_2SiMe_3) salts readily collapse via an alkyl group transfer to form the organodiamidozincates [Zn(R)(NR′−CR═CH−NR′)]$^-$K$^+$ and [Zn(R)(NR′−CH═CH−NR′)]$^-$K$^+$. A thermal alkyl group transfer to the DAB ligand was also observed for a number of neutral [Zn(R)$_2$(R′-DAB)] complexes, resulting in the formation of N- or C-alkylated products.[53,54] Possibly, the reduction products of [Re(R)(CO)$_3$(iPr-DAB)], formulated here as {[Re(CO)$_3$(iPr-DAB)]$^-$···R$^\bullet$}, are also stabilized by an interaction of the R$^\bullet$ radical with the

(51) Vogler, C. Thesis, Universität Stuttgart, 1990.
(52) Wissing, E.; van der Linden, S.; Rijnberg, E.; Boersma, J.; Smeets, W. J. J.; Spek, A. L.; van Koten, G. *Organometallics* **1994**, *13*, 2602.
(53) Klerks, J. M.; Jastrebsky, J. T. B. H.; van Koten, G.; Vrieze, K. *J. Organomet. Chem.* **1982**, *224*, 107.
(54) Kaupp, K.; Stoll, H.; Preuss, H.; Kaim, W.; Stahl, T.; van Koten, G.; Wissing, E.; Smeets, W. J.; Spek, A. L. *J. Am. Chem. Soc.* **1991**, *113*, 5606.

Scheme 3

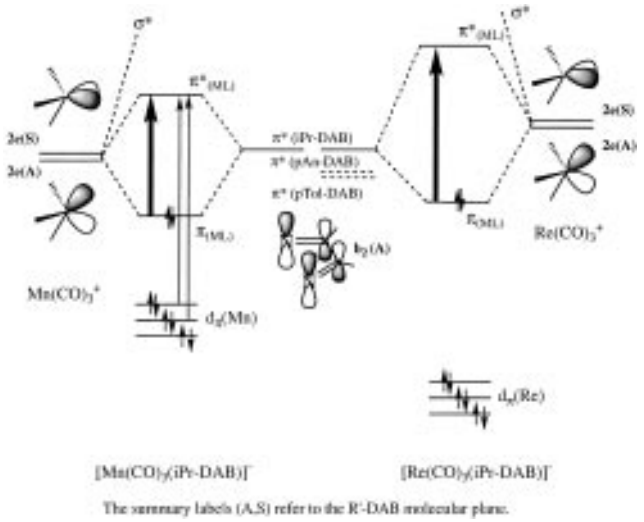

reduced iPr-DAB ligand. In contrast to the stability of {[Re(CO)$_3$(iPr-DAB)]$^-$···R$^\bullet$}, no interaction was observed between the R$^\bullet$ radicals and the anion [Mn(CO)$_3$(iPr-DAB)]$^-$.[44] In the latter anion, however, the actual electron density on the Mn center is higher than those on the Re centers in **14** and especially in **26** and **27** (*vide infra*). Thus, the lower electron density on the Re center and a more diffused character of the d$_\pi$(Re) orbitals may be key factors[55] that allow an interaction between Re and R$^\bullet$ in **15**−**17**, resulting in the reversible nature of the redox couples **3**/**15**, **4**/**16**, and **5**/**17**.

Direct formation of the anionic unit {Re(CO)$_3$(iPr-DAB)}$^-$ upon reduction of [Re(R)(CO)$_3$(iPr-DAB)] was also indicated by the absence of any reaction with PPh$_3$ present in a high excess in the electrolyzed solution. Our results have demonstrated that PPh$_3$ does not coordinate to the anion **14**, but it replaces rapidly the solvent molecules in **9** and **10**, or the Br$^-$ ligand in **12**. We therefore conclude that the reversible one-electron reduction of [Re(R)(CO)$_3$(iPr-DAB)] does not initially lead to [Re(R)(CO)$_3$(iPr-DAB)]$^{\bullet-}$ with properties similar to the radical anion **12**, which would probably immediately react with PPh$_3$ to give the stable radical **11**.

Recently, we studied the bonding situation in the five-coordinate anion [Mn(CO)$_3$(iPr-DAB)]$^-$ [44,56] and compared it with that reported earlier for [Mn(CO)$_3$(DBCat)]$^-$ (DBCat = 3,5-di-*tert*-butylcatecholate dianion).[57] The effect of replacing the central Mn atom by Re is depicted in the qualitative MO diagram for [Re(CO)$_3$(iPr-DAB)]$^-$ (see Scheme 3).

The left part of Scheme 3 shows the frontier MO levels of [Mn(CO)$_3$(iPr-DAB)]$^-$.[44] The MO diagram of [Re(CO)$_3$(iPr-DAB)]$^-$ (**14**) (Scheme 3, right) is constructed on the basis of the spectroscopic and electrochemical evidence obtained in the present study. Notably, a one-electron approach is used, neglecting the configuration and interelectronic interactions. Nevertheless, such an approach is adequate for a qualitative comparison of the bonding and spectroscopic properties of the studied anions [Re(CO)$_3$(R′-DAB)]$^-$.

The energies of the π*(iPr-DAB) frontier orbitals were assumed to be similar in [Mn(CO)$_3$(iPr-DAB)]$^-$ and **14**. One member of the 2e set of the LUMO orbitals of the M(CO)$_3^+$ fragment[58,59] is asymmetric with respect to the iPr-DAB molecular plane (2e(A); see Scheme 3) and π-overlaps with the b$_2$(A) HOMO of the formally (iPr-DAB)$^{2-}$ ligand. This π interaction produces two orbitals, the π_{ML} HOMO and the π^*_{ML} LUMO, that possess significant π-bonding and π-antibonding character, respectively, with regard to the M-N bonds of the M(iPr-DAB) chelate ring. The other empty 2e orbital of the M(CO)$_3^+$ fragment, 2e(S), participates in the σ bonding with the iPr-DAB ligand. The energy difference between the π_{ML} HOMO and π^*_{ML} LUMO can be estimated from the lowest-energy absorption maxima of the [M(CO)$_3$(iPr-DAB)]$^-$ (M = Mn, Re) complexes. The $\pi_{ML}\rightarrow\pi^*_{ML}$ transition is found at λ_{max} = 490 and 440 nm for M = Mn[44] and Re, respectively. However, care must be taken in the comparison of λ_{max} with orbital energy differences since optical excitation also involves contribution from the electron interaction energy associated with the electronic transition, which might be considerably larger for **14** with the heavier Re center. We therefore conclude that the energetic separation of the π_{ML} HOMO and the π^*_{ML} LUMO is slightly higher for **14** in comparison with [Mn(CO)$_3$(iPr-DAB)]$^-$: $\Delta E \leq 1810$ cm^{-1}.

For [Mn(CO)$_3$(iPr-DAB)]$^-$, a second transition was found at λ_{max} = 396 nm, probably from the filled d$_\pi$(Mn) orbitals toward the π^*_{ML} LUMO of the complex.[44,56] The band belonging to this transition was absent in the near-UV−vis spectrum of the anion [Re(CO)$_3$(iPr-DAB)]$^-$. Most likely, the occupied d$_\pi$(Re) orbitals are at lower energy, so that the d$_\pi$(Re)$\rightarrow\pi^*_{ML}$ transition is shifted outside the near-UV−vis range. This assumption is supported by the UV-photoelectron spectral (PES) data reported for the related complexes [Re(Me)(CO)$_3$(iPr-DAB)][31] and [Mn(Me)(CO)$_3$(iPr-DAB)].[45] The set of filled d$_\pi$(Re) orbitals is found at ionization potentials (IP) ranging between 7.23 and 7.79 eV, whereas the set of filled d$_\pi$(Mn) orbitals corresponds to IP = 7.16 eV. Even though these spectra were recorded for neutral hexacoordinate species, the above data show that the energies of the filled d$_\pi$(Re) orbitals are indeed lower (up to 0.63 eV) than those of the filled d$_\pi$(Mn) orbitals. Furthermore, the parent Mn complexes are oxidized at significantly more positive potentials than the Re analogues (*e.g.*: $E_{p,a}$([Mn(Me)(CO)$_3$(iPr-DAB)]) = 0.04V;[44] $E_{p,a}$([Re(Me)(CO)$_3$(iPr-DAB)]) = 0.71 V *vs* Fc/Fc$^+$ in nPrCN).

The character of the π_{ML} HOMO is indirectly revealed from comparison of the average CO force constant k_{av} of the anions. The lower k_{av}, the larger is the M→CO π-back-bonding due to the higher electron density on the metal center. For [Mn(CO)$_3$(DBCat)]$^-$ k_{av} was calculated to be 1498 N m^{-1} (in THF),[57] whereas k_{av} = 1385 N m^{-1} was found for [Mn(CO)$_3$(iPr-DAB)]$^-$.[44] These data, and comparison of the resonance Raman spectra of both Mn complexes,[56,57] led us to conclude that the π_{ML} HOMO of the [Mn(CO)$_3$(iPr-DAB)]$^-$ anion possesses a delocalized d$_\pi$(Mn) + π*(iPr-DAB) character,[56] whereas the π_{ML} HOMO of the DBCat complex has a prevailing contribution from the π* HOMO of the DBCat dianion.[57] This conclusion is also consistent with recent MO calculations on the model complexes [Mn(CO)$_3$(HCat)]$^-$ and [Mn(CO)$_3$(H-DAB)]$^-$.[56] The value of k_{av} = 1408 N m^{-1} for [Re(CO)$_3$(iPr-DAB)]$^-$ resembles more that of [Mn(CO)$_3$(iPr-DAB)]$^-$. The HOMO of [Re(CO)$_3$(iPr-DAB)]$^-$ can thus also be considered as being largely delocalized over the Re(α-diimine) chelate ring. Substitution of the iPr group of the iPr-DAB ligand by an electron-withdrawing aromatic group (pTol, pAn) results in a lower π*(R′-DAB) energy, as was indicated by the more positive reduction potentials of the R′-DAB ligands and the [Re(L′)-

(55) The same reasoning may explain the existence of an equilibrium between [Re(CO)$_3$(R′-DAB)]$^-$ and the six-coordinate anions [Re(nPrCN)(CO)$_3$(R′-DAB)]$^-$, which are unknown for the Mn derivatives.

(56) Hartl, F.; Stufkens, D. J.; Wilms, M. P.; Baerends, E. J. To be published.
(57) Hartl, F.; Stufkens, D. J.; Vlček, A., Jr. *Inorg. Chem.* **1992**, *31*, 1687.
(58) Albright, T. A.; Burdett, J. K.; Whangbo, M. H. *Orbital Interaction in Chemistry*; Wiley Interscience: New York, 1985.
(59) Elian, M.; Hoffman, R. *Inorg. Chem.* **1975**, *14*, 1058.

$(CO)_3$(R′-DAB)]^n (n = 0, L′ = Br^-; n = +1, L′ = nPrCN) complexes (Table 3). The π_{ML} HOMO of the [Re(CO)$_3$(pTol-DAB)]$^-$ and [Re(CO)$_3$(pAn-DAB)]$^-$ anions should therefore possess more R′-DAB character, the bonding situation resembling more that of the [Mn(CO)$_3$(DBCat)]$^-$ anion (Scheme 3). Indeed, the average CO force constant of the latter anions increases with regard to that of [Re(CO)$_3$(iPr-DAB)]$^-$ by 38 N m^{-1} (Table 2).

The lowest energy absorption band of [Mn(CO)$_3$(iPr-DAB)]$^-$ was shown[44,56] to originate from a $\pi_{ML} \rightarrow \pi^*_{ML}$ transition which possesses a delocalized (d_π(Mn) + π^*(iPr-DAB) $\rightarrow$ π^*(iPr-DAB) − d_π(Mn)) character. In the case of [Re(CO)$_3$(iPr-DAB)]$^-$, this $\pi_{ML} \rightarrow \pi^*_{ML}$ transition will also be significantly delocalized over the Re chelate ring, the π_{ML} HOMO and the π^*_{ML} LUMO being considered as d_π(Re) + π^*(DAB) and π^*-(DAB) − d_π(Re), respectively. Unfortunately, resonance Raman spectroscopy could not be applied to gain further information about the character of the $\pi_{ML} \rightarrow \pi^*_{ML}$ transition in [Re(CO)$_3$-(iPr-DAB)]$^-$, since the corresponding absorption band was outside the wavelength region of the exciting laser lines available.

Isostructural and isoelectronic carbonyl complexes of Mn and Re with well-defined oxidation states of the metal center exhibit similar average $\tilde{\nu}$(CO) wavenumbers and hence similar k_{av} values. Typical examples are the complexes [M^{-I}(CO)$_5$]$^-$ and [M^0(CO)$_5$]$_2$,[60] [M^I(nPrCN)(CO)$_3$(iPr-DAB)]$^+$ (k_{av} = 1593 (Mn)[44] and 1577 (Re) N m^{-1} in nPrCN at 293 K), and [M^I(THF)(CO)$_3$-(DBSQ)] (DBSQ = 3,5-di-*tert*-butyl-1,2-benzosemiquinone radical anion) (k_{av} = 1555 (Mn)[57] and 1527 (Re)[61] N m^{-1} in THF at 293 K). The last two examples indicate that the M $\rightarrow$ CO π-back-donation in the complexes [M^I(L′)(CO)$_3$(LL)]$^{+/0}$ (M = Mn, Re; L′ = weak donor solvent, Otf^-, PR_3; LL = α-diimine, semiquinone radical anion) is generally somewhat stronger for M = Re. (However, there is also a σ contribution that might be quite different for Mn and Re, to account for the above differences in k_{av}.) This situation evidently does not apply for the studied anions [M(CO)$_3$(iPr-DAB)]$^-$ where k_{av} is significantly *higher* for M = Re (*vide supra*), indicating thus that the Mn -anionic species has a more electron-rich metal center. The k_{av} values of the latter anions might point to their formulation as [M^0(CO)$_3$(iPr-DAB)]$^-$ in agreement with k_{av} = 1498 N m^{-1} [57] for [Mn^I(CO)$_3$(DBCat)]$^-$ and k_{av} = 1320 N m^{-1} for [Mn^{-I}(CO)$_3$(dppe)]$^-$.[62] In fact, definition of nonintegral oxidation states of M would be necessary to reflect the higher electron density on the Mn center with respect to **14**. Such an attempt is however meaningless in this case where the strong delocalization of the π-electron density over the M(iPr-DAB) chelate ring demands us to abandon the localized-valence concept.[63]

The proposed description of the delocalized π bonding in [Re(CO)$_3$(R′-DAB)]$^-$ (Scheme 3) may generally be applied for all five-coordinate anions [Re(CO)$_3$(α-diimine)]$^-$ reported so far.[10,12,17,46] The lower k_{av} values (in N m^{-1}) then reflect the increasing delocalization of the added electrons over the (CO)$_3$-Re(α-diimine) moiety with the increasing π-donor character of the reduced α-diimine ligand[26] in the order dpp (1444)[10] < pTol-DAB (1442) ∼ pAn-DAB (1441) < *N*,*N*′-dapa (1439)[10] << bpy (1425)[10] < iPr-PyCa (1422)[10] << iPr-DAB (1408) ∼ dmbpy (1408).[12]

Conclusions

This study showed that the one-electron reduction of [Re-(Br)(CO)$_3$(R′-DAB)] resulted in the establishment of an equilibrium between [Re(Br)(CO)$_3$(R′-DAB)]$^{\bullet-}$ and [Re(nPrCN)-(CO)$_3$(R′-DAB)]$^\bullet$. The position of the equilibrium, as determined from the IR OTTLE data, was significantly influenced by the R′ substituent on the R′-DAB ligand and by the temperature. In general, the more electron-withdrawing R′, the more stable were the radical anions.

The complexes [Re(R)(CO)$_3$(iPr-DAB)] (R = Me, Et, Bz) could be reduced with one electron to give the radical anionic products {[Re(CO)$_3$(iPr-DAB)]$^-$···R$^\bullet$}, electronically resembling the five-coordinate anion [Re(CO)$_3$(iPr-DAB)]$^-$ formed upon the one-electron reduction of [Re(Br)(CO)$_3$(iPr-DAB)]$^{\bullet-}$ and [Re(L′)(CO)$_3$(iPr-DAB)]$^\bullet$ (L′ = PPh_3, nPrCN). The reduction of [Re(R)(CO)$_3$(iPr-DAB)] was found to be both chemically and electrochemically fully reversible, indicating that the R$^\bullet$ radical remained in the vicinity of the Re center.

The qualitative description of the MO diagram for the five-coordinate anion [Re(CO)$_3$(iPr-DAB)]$^-$ showed that the π bonding in the Re(iPr-DAB) chelate ring is strongly delocalized. The lowest energy $\pi_{ML} \rightarrow \pi^*_{ML}$ transition in this compound can be considered as having a largely mixed (d_π(Re) + π^*-(DAB) $\rightarrow$ π^*(DAB) − d_π(Re)) character. The proposed bonding situation may also be applied for other five-coordinate anions [Re(CO)$_3$(α-diimine)]$^-$, taking into account differences in the basicity and donor properties of the reduced α-diimine ligands.

Acknowledgment. The Netherlands Foundation of Chemical Research (SON) and the Netherlands Organisation for the Advancement of Pure Science (NWO) are thanked for their financial support.

Supporting Information Available: Figures 2, 3, 6 and 8, showing UV−vis spectra and additional IR spectra and cyclic voltammograms (5 pages). Ordering information is given on any current masthead page.

IC9600947

(60) van der Graaf, T.; van Rooy, A.; Stufkens, D. J.; Oskam, A. *Inorg. Chim. Acta* **1991**, *187*, 133.
(61) Hartl, F.; Vlček, A., Jr. *Inorg. Chem.* **1992**, *31*, 2869.
(62) Kuchynka, D. J.; Amatore, C.; Kochi, J. K. *J. Organomet. Chem.* **1987**, *328*, 133.
(63) Vlček, A., Jr. *Comments Inorg. Chem* **1994**, *16*, 207.